AGU100 ADVANCING EARTH AND SPACE SCIENCE

Geophysical Research Letters

RESEARCH LETTER
10.1029/2019GL084331

Key Points:
- Maximum sprite streamer luminosity near stratopause detected
- Sprite morphology attributed to surge of intracloud lightning activity

Correspondence to:
M. Füllekrug,
eesmf@bath.ac.uk

Citation:
Füllekrug, M., Nnadih, S., Soula, S., Mlynarczyk, J., Stock, M., Lapierre, J., & Kosch, M. (2019). Maximum sprite streamer luminosity near the stratopause. *Geophysical Research Letters*, *46*, 12,572–12,579. https://doi.org/10.1029/2019GL084331

Received 28 JUN 2019
Accepted 19 SEP 2019
Accepted article online 16 OCT 2019
Published online 11 NOV 2019

Maximum Sprite Streamer Luminosity Near the Stratopause

Martin Füllekrug[1], Stanislaus Nnadih[2,3,4], Serge Soula[5], Janusz Mlynarczyk[6], Micheal Stock[7], Jeff Lapierre[7], and Michael Kosch[2,8,9,10]

[1]Centre for Space, Atmospheric and Oceanic Science, Department of Electronic and Electrical Engineering, University of Bath, Bath, UK, [2]South African National Space Agency, Hermanus, South Africa, [3]SpaceLab, Department of Electrical Engineering, University of Capetown, Capetown, South Africa, [4]Now at African Regional Centre for Space Science and Technology Education in English, Ife, Nigeria, [5]Laboratoire d'Aérologie, Université Paul Sabatier Toulouse III, Toulouse, France, [6]Department of Electronics, AGH University of Science and Technology, Krakow, Poland, [7]Earth Networks, Germantown, MD, USA, [8]Department of Physics, Lancaster University, Lancaster, UK, [9]Physics and Astronomy, University of the Western Cape, Bellville, South Africa, [10]School of Chemistry and Physics, University of KwaZulu-Natal, Westville, South Africa

Abstract Sprites are composed of numerous streamers which exhibit transient luminosities in the upper middle atmosphere above thunderclouds after initiation by an intense positive lightning discharge, often followed by lightning continuing current. Here we report the discovery of a sprite which exhibits its main luminosity near the stratopause. This novel phenomenon is attributed to a sudden surge of intracloud lightning leader activity, based on a rigorous analysis of our observed electromagnetic waveforms. Each lightning leader discharge causes an additional electric field that generates a small amount of electromagnetic energy near the stratopause and thereby contributes to the overall sprite luminosity morphology. The observation of sprite streamers near the stratopause is important because it is relevant for the ongoing assessment of the lightning impact on N_2 and CO_2 with emissions from the near to far infrared part of the spectrum.

1. Introduction

Sprites are transient luminous events above thunderclouds that occur mainly after intense positive lightning discharges and occasionally after negative lightning discharges. The typical morphology of sprites originally distinguished the central sprite head around ~70–75 km height, the hair above ~75–90 km, and downward extending tendrils from ~40–70 km height (e.g., Sentman et al., 1995, Figure 2). Yet sprites are composed of numerous individual streamers such that a morphological classification can also be based on the underlying physical processes, that is, the streamer region from ~45–75 km height, the transition region from ~75–85 km height, and the diffuse region from ~85–95 km (e.g., Pasko, 2010, Figure 4, and references therein). It is common practice to refer to the most luminous part of sprites as the body (e.g., Bor, 2013, and references therein) which normally coincides with the head, or transition region, of sprites.

The morphological properties of optical sprite observations are commonly attributed to the specific characteristics of the sprite producing lightning discharges. For example, the vast majority of sprites are caused by intense positive lightning discharges (Boccippio et al., 1995; Pasko, 2010, and references therein) followed by a lightning continuing current (Cummer et al., 1998; Pasko et al., 1998; Reising et al., 1996) with a large charge moment change (Cummer & Stanley, 1999; Cummer & Füllekrug, 2001). On occasion, sprites are initiated by negative lightning discharges (Barrington-Leigh & Inan, 1999) as confirmed by detailed experimental observations (Boggs et al., 2016; Chen et al., 2019; Lu et al., 2012) and supported by corresponding theoretical studies (Liu et al., 2016; Qin et al., 2012). Column sprites are attributed to the large positive peak current of lightning discharges while carrot sprites tend to be associated with extended intracloud lightning activity which neutralises large quantities of charge inside the thundercloud (e.g., Qin et al., 2013; van der Velde et al., 2006, and references therein). In particular, sprites with a long delay after the initial positive lightning discharge are attributed to intense intracloud lightning activity (e.g., Bell et al., 1998; Lu et al., 2013; Marshall et al., 2007, and references therein) where long delayed sprites typically initiate at ~5 km lower heights in the upper mesosphere when compared to short delayed sprites (Li et al., 2008). Originally, the

intracloud lightning activity associated with sprites has been described as "spider lightning" (Lyons, 1996). More recently, the in-cloud leader growth associated with positive lightning continuing current was studied in detail (Lapierre et al., 2017). Intracloud lightning activity has been observed at remote distances as "sferic clusters," or "radio noise," in the extremely low frequency range (30 Hz to 3 kHz) (Ohkubo et al., 2005), the very low frequency range (3–30 kHz) (Johnson & Inan, 2000; Marshall et al., 2007) and in the low frequency range (30–300 kHz) as a quick succession of radio pulses (Füllekrug et al., 2013; Figure 4). At short range distances, the source locations of radio pulses from intracloud lightning leader discharges can be mapped in two or three dimensions by low frequency interferometry (e.g., Bitzer et al., 2013; Füllekrug et al., 2013; Lyu et al., 2014) and more commonly by very high frequency (30–300 MHz) interferometry with lightning mapping arrays (e.g., Boggs et al., 2016; Lu et al., 2012, 2013, and references therein). Most recently, the astronomical radio telescope LOw Frequency ARray (LOFAR) has been used to study intracloud lightning in unprecedented detail (e.g., Hare et al., 2019, and references therein).

However, the morphological differences of sprite luminosities associated with varying degrees of intracloud lightning activity, positive lightning peak current, and subsequent continuing current are not well documented. For example, the tendrils in the streamer zone are on occasion optically very bright (e.g., Soula et al., 2017, Figure 5a, F41, Mlynarczyk et al., 2015, Figure 3, F7G). These sprite streamer luminosities near the stratopause are important because they reflect the emissions from vibrational states of N_2 and CO_2 from the near to far infrared part of the spectrum (e.g., Bucsela et al., 2003; Gordillo-Vazquez et al., 2012; Kanmae et al., 2007; Picard et al., 1997; Parra-Rojas et al., 2015; Romand et al., 2018, and references therein). In particular, it is predicted that intermediate (50 ms) and long (100 ms) duration current flows associated with lightning discharges inside thunderclouds assist to sustain the vibrational states of CO_2 (Parra-Rojas et al., 2015). These simulations extend from the upper mesosphere down to 50 km height near the stratopause. This letter reports a detailed comparison of the morphology of a sprite with its main luminosity near the stratopause and another sprite with its main luminosity in the upper mesosphere. The properties of the causative lightning discharges are quantified by use of novel sprite observations in South Africa (Nnadih et al., 2018).

2. Observations

A large front of numerous mesoscale convective systems extends from eastern South Africa to northern Namibia over $\%500 \times 2{,}000$ km^2 at 19:45 Coordinated Universal Time (UTC) on 24 January 2017 (Figure 1, left). The cloud top brightness temperatures reported by the geostationary satellite Meteosat reach down to ~ -80°C and indicate a tropopause near $\sim$ 15–16 km height inferred from a radiosonde ascent from Upington at 00 UTC on 25 January (University of Wyoming, 2019), $\sim$ 350 km south of the sprite producing lightning discharges. This major front of convective instability propagates north-eastward during the night and produces numerous lightning discharges and at least 24 sprites. The average cloud top brightness temperature at the 17 known locations of sprite producing lightning discharges reported by the Earth Networks Total Lightning Network is -70 ± 9°C with corresponding heights ranging from $\sim$ 12–16 km. A similar result is obtained when the lightning locations reported by the lightning detection network of the South African Weather Service are used. Around $\sim$ 50 % of the sprite producing lightning discharges are located in the convective region of the mesoscale convective system with brightness temperatures from −70°C to −80°C. The remaining $\sim$ 50 % of the sprite producing lightning discharges occur at larger temperatures $>$ −70° where it cannot be determined from temperatures alone whether they are located in the convective or stratiform region of the mesoscale convective system.

2.1. Optical Video Imagery

Optical sprite observations are conducted with a low-light video camera located at the South African Astronomical Observatory (−32.38° S, 20.81° E) from 18:45-21:00 UTC. The camera points toward the north-east at one particular mesoscale convective system ~800 km away which produces at least 24 sprites during the observation period. The camera system consists of a Watec 910Hx which is equipped with an 8 mm f1.8 lens with a field of view of $\sim$ 22.3° in the horizontal and $\sim$ 14.3° in the vertical direction. The video recordings are performed with a fixed gain and the default gamma factor 0.45. The video images are initially acquired with a time interval of 40 ms between consecutive images taken at a frame rate of 25 fps. The temporal resolution of the video sequence is increased to 20 ms by deinterlacing the recorded images into two images, one with odd scan lines and one with even scan lines. Subsequently, the sprite images are extracted from the original recordings by use of standard image processing methods (Füllekrug et al., 2013, section 2, paragraph 4).

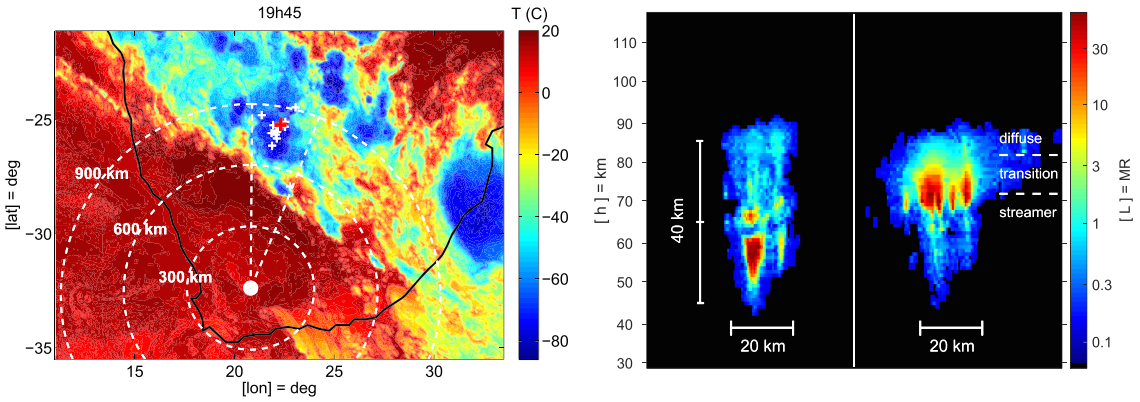

Figure 1. Sprite observations in South Africa. (left). The South African Astronomical Observatory (dot) hosts a sprite observing low-light video camera with a horizontal field of view ~ 22.3° (dashed lines). Around ~800 km to the north-east of the video camera (dashed circles) numerous sprite producing lightning discharges occur (white pluses) and cause two particularly luminous sprites (superposed red pluses). All sprites occur within large scale thunderstorm activity as inferred from the cloud top temperatures recorded on the geostationary satellite Meteosat (color scale). (right). The two most luminous sprites differ significantly. The first sprite on the left exhibits its largest luminosity with corresponding streamer densities near the stratopause ~50–60 km height, while the second sprite on the right exhibits its largest luminosity with corresponding streamer densities in the upper mesosphere ~70–80 km height. The observed differences are attributed to the characteristic properties of the causative lightning discharges.

Finally, the luminosity for each pixel is inferred from the image count multiplied with the sensitivity of the camera obtained from the brightness of known stars in the field of view. The two most luminous sprites that occurred during the night are recorded in short succession at 19:34:27.050 UTC and at 19:47:42.962 UTC. Both sprites are recorded on one single video image of 20 ms duration and might consist of several nearby sprite elements. The corresponding video images of these two sprites differ significantly (Figure 1, right). The first sprite on the left exhibits its maximum luminosity near the stratopause from ~50–60 km height and the second sprite on the right exhibits its maximum luminosity in the upper mesosphere from ~70–80 km height. The heights h of the sprite luminosities are calculated here from the law of sines

$$\frac{\sin(\vartheta + \pi/2)}{a + h} = \frac{\sin \alpha}{a + e}, \tag{1}$$

where ϑ is the elevation angle under which the sprite luminosity is seen with respect to the horizontal direction, $a = 6,371$ km is the equivolumetric radius of the Earth, h is the height of the sprite luminosity, α is the angle subtended from the sprite luminosity to the video camera with respect to the vertical direction, and $e = 1,764$ m is the elevation of the camera above sea level at the South African Astronomical Observatory. The unknown angle α can be calculated from the other two known angles $\alpha = \pi - \vartheta - \pi/2 - \gamma = \pi/2 - \vartheta - d/a$, where $\gamma = d/a$ is the central angle determined by the great circle distance d between the sprite producing lightning discharge and the video camera measured along the surface of the Earth. Solving equation 1 for the height of the sprite luminosity then results in

$$h = \frac{(a + e)\sin(\vartheta + \pi/2)}{\sin(\pi/2 - \vartheta - d/a)} - a, \tag{2}$$

where the uncertainty of the height calculation is mainly determined by the measurement uncertainty of the elevation angle when the distance between the sprite and the video camera is known. This distance is approximated here by use of the positive lightning discharge location preceding the optical sprite observation, as reported by the lightning detection network of the South African Weather Service with an uncertainty <1 km indicated by the location error ellipse. However, sprites can occasionally be displaced by ~30–40 km from the sprite producing lightning discharge (e.g., Soula et al., 2017, and references therein). As a result, a conservative estimate for the height uncertainty can be obtained from the average distance ~ 800 km between the video camera and the sprite producing lightning discharges with known locations and a lateral uncertainty ~ 30 km. The resulting estimate for the height uncertainty is then ~ 5 km at 90 km and ~ 3.5 km at 45 km height. These uncertainties are considered to be reasonable estimates because larger uncertainties, say beyond ±10 km height, would result in unusual (large or small) terminal heights of the diffuse region of the observed sprites.

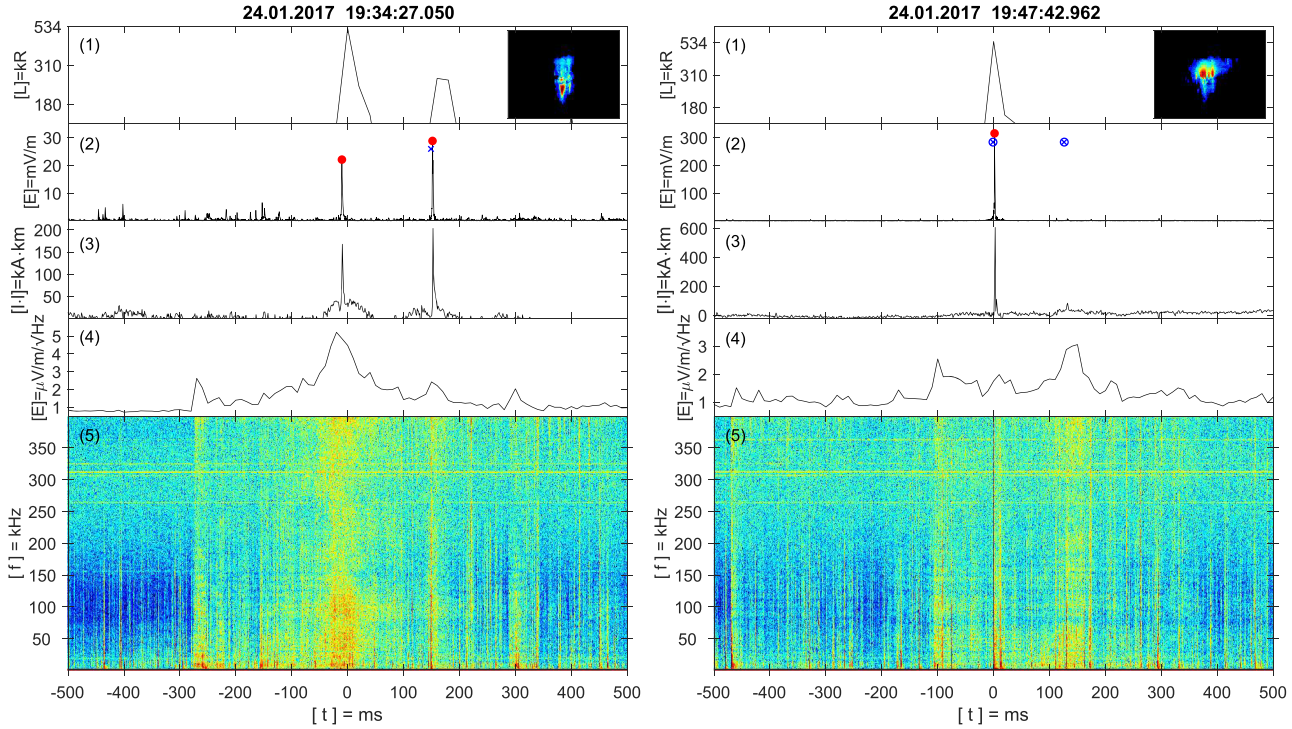

Figure 2. Comparison of the two lightning discharges that cause the most luminous sprites. (left). The sprite with the largest density of streamers near the stratopause reaches a luminosity of ~530 kR (panel 1). The sprite is caused by a positive lightning discharge (~4 Hz–2 kHz) with a relatively small peak electric field strength envelope ~20 mV/m (red dot in panel 2). The current moment of the lightning discharge is ~150 kA·km (panel 3), and it is embedded in a surge of ~500ms long intracloud lightning activity (panels 4 and 5). A secondary column sprite occurs ~150 ms after the first sprite, caused by a positive lightning discharge reported by the South African Weather Service (blue cross). (right). The sprite with the largest density of streamers in the upper mesosphere also reaches a luminosity of ~530 kR (panel 1). Yet the sprite is caused by a tenfold more intense positive lightning discharge with a peak electric field strength envelope ~300 mV/ms (panel 2) which was also reported by Earth Networks lightning detection network (blue circles). The measured current moment of the positive lightning discharge ~600 kA·km is ~4 times larger when compared to the first sprite causing lightning discharge (panel 3). This positive lightning discharge is embedded in two times less intense intracloud lightning activity (panels 4 and 5).

2.2. Electromagnetic Waveforms

The morphological difference of the two sprites with a larger streamer density near the stratopause and in the upper mesosphere is attributed to the characteristic properties of the corresponding causative lightning discharges. These properties are determined from remote sensing of the electromagnetic waves emitted by the lightning discharges. Electric field strengths are recorded with a wideband digital low-frequency radio receiver from ~4 Hz to ~400 kHz with a sampling frequency of 1 MHz (Füllekrug, 2010) at the South African Astronomical Observatory and extremely-low frequency magnetic field variations from ~0.03 Hz to ~300 Hz are recorded with a sampling frequency of 887 Hz ~8,270 km away from the sprites at Hylaty (49.20° N, 22.54° E) in the sparsely populated Bieszczady Mountains of Poland (Kulak et al., 2014).

2.2.1. Lightning Causing Maximum Sprite Luminosity Near the Stratopause

The sprite with the largest streamer density near the stratopause reaches an average luminosity ~530 kR (Figure 2, left, panel 1). The sprite is initiated by a positive lightning discharge with a measured peak electric field strength envelope ~22 mV/m in the frequency range from 4 Hz to 2 kHz (Figure 2, left, panel 2). Around ~150 ms later, a secondary column sprite is initiated by a subsequent positive lightning discharge with a peak electric field strength envelope ~29 mV/m. The positive polarity of both radio pulses is determined by the instantaneous polarity (Taner et al., 1979). The second lightning discharge is a positive lightning discharge with a peak amplitude of ~35 kA as reported by the lightning detection network of the South African Weather Service. The magnetic field recordings are used to calculate the lightning current moment (Mlynarczyk et al., 2015, and references therein) which exhibits the same two pulses from the positive lightning discharges (Figure 2, left, panel 3). The current moment measurement of the first lightning discharge is used to calculate the instantaneous charge moment change ~269 C·km and the total charge moment change ~325 C·km which are both near the approximate limit ~ 300 ± 100 C·km required for sprite initiation (Qin et al., 2012, and references therein). The current moment pulse from the positive lightning

discharge is superimposed on a more slowly varying "hump" from −50 ms to +50 ms. This hump is paralleled by a surge of intracloud lightning activity which is recorded by the nearby electric field measurements as background noise (Figure 2, left, panel 4). This background noise results from the fast succession of consecutive lightning leader pulses that can occur with a repetition rate of ∼10–20 per ms (Füllekrug et al., 2013). It is therefore possible to separate the signal of intracloud lightning leader pulses from the signal of a return stroke with a duration ∼ 1 ms by using the minimum electric field variability $\Delta E_{\min}$ within 10 ms long time intervals selected from successive dynamic spectra calculated with a temporal resolution of 1 ms (Füllekrug et al., 2013). Because the intensity of radio pulses is roughly log-normal distributed, the electric field variability $\Delta E_{1\ \mathrm{ms}}$ during 1 ms is calculated by use of the logarithmic mean

$$\mu = \frac{1}{N}\sum_{k=1}^{N}\log_{10} S(f_k), \tag{3}$$

where $S(f_k)$ are the spectral amplitude densities at $N = 400$ frequencies f_k from 1–400 kHz separated by 1 kHz (Figure 2, left, panel 5) such that the electric field variability is given by $\Delta E_{1\ \mathrm{ms}} = 10^{\mu}$. The minimum electric field variability $\Delta E_{\min}$ is then the smallest $\Delta E_{1\ \mathrm{ms}}$ within each 10 ms long time interval, and it characterizes intracloud lightning activity because return strokes have effectively been removed.

2.2.2. Lightning Causing Maximum Sprite Luminosity in the Upper Mesosphere

The sprite with the largest streamer density in the upper mesosphere reaches an average luminosity ∼530 kR (Figure 2, right, panel 1), that is incidentally similar to the sprite with the largest streamer density near the stratopause. Yet, the peak electric field strength envelope of the positive lightning discharge ∼315 mV/m is ∼14 times larger than the peak electric field strength envelope of the lightning discharge which causes the largest streamer density near the stratopause (Figure 2, right, panel 2). The measured peak current of the positive lightning discharge is +115 kA as reported by the lightning detection network of the South African Weather Service. Around ∼127 ms later, another positive lightning discharge with a peak current ∼15 kA occurs, but it does not produce a sprite. The measurements of the instantaneous charge moment change ∼901 C·km, and the total charge moment change ∼1,190 C·km are ∼3 times larger than for the sprite with the largest streamer density near the stratopause (Figure 2, right, panel 3). At the same time, the intracloud lighting activity measured by the background noise is ∼2 times smaller than for the sprite with the largest streamer density near the stratopause (Figure 2, right, panels 4 and 5). These results strongly suggest that the luminosity of streamers near the stratopause is more sensitive to intracloud lightning activity, possibly associated with a large charge moment change accumulated over a relatively long timescale, while the luminosity of streamers in the upper mesosphere is more sensitive to the impulsiveness of the initial charge transfer with a consecutive large charge moment change.

The two sprites reported here with extreme opposite characteristics occurring within ∼13–14 min of each other are a rather serendipitous discovery. Another sprite group with the largest luminosity of sprite streamers near the stratopause was recorded during the same night at 20:04:16.801 UTC, and similar examples were also observed during more recent field work in South Africa. However, for a statistical study of maximum streamer luminosities near the stratopause many more examples would be needed, as the vast majority of sprites exhibit a large degree of variability between the peak current of the positive lightning discharge, the instantaneous and total charge moment change and the intracloud lightning leader discharge activity.

2.3. Summary of the Experimental Observations

Our experimental observations can be summarized as follows:

1. Two particular positive lightning discharges that are located in a mesoscale convective system occur within ∼13–14 min of each other.
2. Both lightning discharges cause sprites as their instantaneous and total charge moment changes exceed the required theoretical sprite initiation threshold ∼ 300 ± 100 C·km.
3. Both sprites extend from ∼45–90 km height as recorded on a single video image that integrates over a time interval of 20 ms such that no information on the initiation heights of the sprites, and their temporal development can be inferred.
4. One sprite exhibits its maximum streamer luminosity near the stratopause from ∼50–60 km height. This sprite is caused by a charge moment change ∼ 300 ± 30 C·km embedded in a surge of ∼500 ms long intracloud lightning leader discharge activity.

5. The other sprite exhibits its maximum streamer luminosity in the upper mesosphere from ~70–80 km height. This sprite is caused by a charge moment change ~ 1,050 ± 150 C·km associated with ~2 times weaker intracloud lightning leader discharge activity that lasts for ~300 ms.

3. Interpretation

To the best of our knowledge, there are currently no sprite simulations that predict maximum streamer luminosities near the stratopause. As a result, our interpretation is based on the straightforward discrimination between the experimental observations of the two sprites with maximum streamer luminosities near the stratopause and in the upper mesosphere. The charge moment changes of both positive lightning discharges initiate the two sprites with reduced electric fields that cause streamer luminosities extending from ~45–90 km height. Consequently, the difference in sprite morphology, that is, the maximum streamer luminosity near the stratopause, is attributed to an additional electric field superimposed on the breakdown electric field caused by the charge moment changes of the positive lightning discharges. The corresponding surge of intracloud lightning leader discharges suggests that the physical cause of this additional electric field resides inside the thundercloud. In particular, two potential mechanisms might contribute to the additional electric field: (1) The intracloud lightning leader discharges neutralize laterally distributed charge centers within the thundercloud over a relatively long timescale which results in a quasi-static electric field change with a multipole character. Higher-order multipole fields fall off faster with distance when compared to lower order multipole fields and might thereby contribute to the additional electric field required to explain the enhanced streamer luminosity near the stratopause. (2) It was previously proposed that the combined radiated electric fields of numerous small intracloud lightning leader discharges contribute to the sprite morphology (e.g., Ohkubo et al., 2005; Valdivia et al., 1997). In this model, the current moment change of each intracloud lightning leader discharge causes a horizontally oriented electric dipole with a radiation pattern that falls off faster with vertical distance than the electric field from a monopole. However, this model intended to explain the filamentary structure of sprites in the upper mesosphere, rather than relative sprite streamer luminosity enhancements near the stratopause.

In either of the two cases discussed above, each intracloud lightning leader discharge contributes an additional electric field that is larger near the stratopause when compared to the upper mesosphere. This additional electric field enhancement thereby results in a quasi-static Joule heating of the atmosphere above the thundercloud (Füllekrug et al., 2006) and a corresponding relative increase of the streamer luminosity near the stratopause when compared to the upper mesosphere. In contrast, the relatively large sprite streamer luminosity in the upper mesosphere is produced by the superposition of sprite streamers and the diffuse halo (Pasko et al., 2013, Figure 9) that is caused by the impulsiveness of the initial charge transfer with a consecutive large charge moment change of the sprite producing positive lightning discharge.

4. Summary

This letter reports the serendipitous discovery of two sprites within a ~13–14 min time interval which differ significantly in their optical morphology: one sprite exhibits its largest luminosity in the upper mesosphere while the other sprite exhibits its largest luminosity near the stratopause. It is proposed that this novel phenomenon of maximum sprite luminosity near the stratopause can be explained by a surge of intracloud lightning leader discharges following a relatively weak positive lightning discharge with a charge moment near the sprite initiation threshold. In this picture, each intracloud lightning leader discharge causes an additional electric field that generates a small amount of electromagnetic energy in the atmosphere above the thundercloud and thereby contributes to the observed luminosity near the stratopause. The described impact of intracloud lightning leader discharges on the stratopause is important because it can be relevant for the ongoing quantitative assessment of the vibrational states of N_2 and CO_2 with emissions from the near to far infrared part of the spectrum, as described in the introduction (section 1).

Acknowledgments
This project was sponsored by the Royal Society (UK) Grant NMG/R1/180252, National Research Foundation (South Africa) Grant 105535, National Science Center (Poland) Grant 2015/19/B/ST10/01055, and the Natural Environment Research Council (UK) under Grants NE/L012669/1 and NE/H024921/1. M.F. developed the concept for this letter and wrote it, conducted the data analysis, and contributed to the measurements led by S.N. and M.K. S.N., and M.K. also advised on the optical data analysis. S.S. contributed meteorological information, and J.M. provided magnetic field observations and their inversion. M.S. and J.L. communicated Earth Networks lightning location data for comparison. M.F. acknowledges helpful discussions with Adrian Evans, Corwin Wright, and Frank Tschepke. The authors wish to thank the South African Astronomical Observatory for their logistic support and the South African Weather Service for limited access to their lightning location data. The data used for this publication will be available from https://doi.org/10.15125/BATH-00669.

References

Barrington-Leigh, C., & Inan, U. (1999). Sprites triggered by negative lightning discharges. *Geophysical Research Letters*, *26*(24), 3605–3608. https://doi.org/10.1029/1999GL010692

Bell, T., Reising, S., & Inan, U. (1998). Intense continuing currents following positive cloud-to-ground lightning associated with red sprites. *Geophysical Research Letters*, *25*(8), 1285–1288. https://doi.org/10.1029/98GL00734

Bitzer, P., Christian, H., Stewart, M., Burchfield, J., Podgorny, S., Corredor, D., et al. (2013). Characterization and applications of VLF/LF source locations from lightning using the Huntsville Alabama Marx Meter Array. *Journal of Geophysical Research: Atmospheres*, *118*, 3120–3138. https://doi.org/10.1002/jgrd.50271

Boccippio, D., Williams, E., Heckman, S., Lyons, W., Baker, I., & Boldi, R. (1995). Sprites, ELF transients, and positive ground strokes. *Science*, *269*, 1088–1091. https://doi.org/10.1126/science.269.5227.1088

Boggs, L., Liu, N., Splitt, M., Lazarus, S., Glenn, C., Rassoul, H., & Cummer, S. (2016). An analysis of five negative sprite-parent discharges and their associated thunderstorm charge structures. *Journal of Geophysical Research: Atmospheres*, *121*, 759–784. https://doi.org/10.1002/2015JD024188

Bor, J. (2013). Optically perceptible characteristics of sprites observed in Central Europe in 2007-2009. *Journal of Atmospheric and Solar-Terrestrial Physics*, *92*, 151–177. https://doi.org/10.1016/j.jastp.2012.10.008

Bucsela, E., Morrill, J., Heavner, M., Siefring, C., Berg, S., Hampton, D., et al. (2003). $N_2(B^3\Pi_g)$ and $N_2^+(A^2\Pi_u)$ vibrational distributions observed in sprites. *Journal of Atmospheric and Solar-Terrestrial Physics*, *65*, 583–590. https://doi.org/10.1016/S1364-6826(02)00316-4

Chen, A., Chen, H., Chuang, C., Cummer, S., Lu, G., Fang, H., et al. (2019). On negative sprites and the polarity paradox. *Geophysical Research Letters*, *46*, 9370–9378. https://doi.org/10.1029/2019GL083804

Cummer, S., & Füllekrug, M. (2001). Unusually intense continuing current in lightning produces delayed mesospheric breakdown. *Geophysical Research Letters*, *28*(3), 495–498. https://doi.org/10.1029/2000GL012214

Cummer, S., Inan, U., Bell, T., & Barrington-Leigh, C. (1998). ELF radiation produced by electrical currents in sprites. *Geophysical Research Letters*, *25*(8), 1281–1284. https://doi.org/10.1029/98GL50937

Cummer, S., & Stanley, M. (1999). Submillisecond resolution lightning currents and sprite development: Observations and implications. *Geophysical Research Letters*, *26*(20), 3205–3208. https://doi.org/10.1029/1999GL003635

Füllekrug, M., Ignaccolo, M., & Kuvshinov, A. (2006). Stratospheric joule heating by lightning continuing current inferred from radio remote sensing. *Radio Science*, *41*, RS2S19. https://doi.org/10.1029/2006RS003472

Füllekrug, M., Mezentsev, A., Soula, S., van der Velde, O., & Evans, A. (2013). Illumination of mesospheric irregularity by lightning discharge. *Geophysical Research Letters*, *40*, 6411–6416. https://doi.org/10.1002/2013GL058502

Füllekrug, M., Wideband digital low-frequency radio receiver (2010). *Measurement Science and Technology*, *21*(15901), 1–9. https://doi.org/10.1088/0957-0233/21/1/015901

Gordillo-Vazquez, F. J., Luque, A., & Simek, M. (2012). Near infrared and ultraviolet spectra of TLEs. *Journal of Geophysical Research*, *117*, A05329. https://doi.org/10.1029/2012JA017516

Hare, B., Scholten, O., Dwyer, J., Trinh, T., Buitink, S., ter Veen, S., et al. (2019). Needle-like structures discovered on positively charged lightning branches. *Nature*, *568*, 360–363. https://doi.org/10.1038/s41586-019-1086-6

Johnson, M., & Inan, U. (2000). Sferic clusters associated with early/fast VLF events. *Geophysical Research Letters*, *27*(9), 1391–1394. https://doi.org/10.1029/1999GL010757

Kanmae, T., Stenbaek-Nielsen, H., & McHarg, M. (2007). Altitude resolved sprite spectra with 3 ms temporal resolution. *Geophysical Research Letters*, *34*, L07810. https://doi.org/10.1029/2006GL028608

Kulak, A., Kubisz, J., Klucjasz, S., Michalec, A., Mlynarczyk, J., Nieckarz, Z., et al. (2014). Extremely low frequency electromagnetic field measurements at the Hylaty station and methodology of signal analysis. *Radio Science*, *49*, 361–370. https://doi.org/10.1002/2014RS005400

Lapierre, J., Sonnenfeld, R., Stock, M., Krehbiel, P., Edens, H., & Jensen, D. (2017). Expanding on the relationship between continuing current and in-cloud leader growth. *Journal of Geophysical Research: Atmospheres*, *122*, 4150–4164. https://doi.org/10.1002/2016JD026189

Li, J., Cummer, S., Lyons, W., & Nelson, T. (2008). Coordinated analysis of delayed sprites with high-speed images and remote electromagnetic fields. *Journal of Geophysical Research*, *113*, D20206. https://doi.org/10.1029/2008JD010008

Liu, N., Boggs, L., & Cummer, S. (2016). Observation-constrained modeling of the ionospheric impact of negative sprites. *Geophysical Research Letters*, *43*, 2365–2373. https://doi.org/10.1002/2016GL068256

Lu, G., Cummer, S., Blakeslee, R., Weiss, S., & Beasley, W. (2012). Lightning morphology and impulse charge moment change of high peak current negative strokes. *Journal of Geophysical Research*, *117*, D04212. https://doi.org/10.1029/2011JD016890

Lu, G., Cummer, S. A., Li, J., Zigoneanu, L., Lyons, W. A., Stanley, M. A., et al. (2013). Coordinated observations of sprites and in-cloud lightning flash structure. *Journal of Geophysical Research: Atmospheres*, *118*, 6607–6632. https://doi.org/10.1002/jgrd.50459

Lyons, W. (1996). Sprite observations above the U.S. high plains in relation to their parent thunderstorm systems. *Journal of Geophysical Research*, *101*(23), 29,641–29,652. https://doi.org/10.1029/96JD01866

Lyu, F., Cummer, S. A., Solanki, R., Weinert, J., McTague, L., Katko, A., et al. (2014). A low-frequency near-field interferometric-TOA 3-D Lightning Mapping Array. *Geophysical Research Letters*, *41*, 7777–7784. https://doi.org/10.1002/2014GL061963

Marshall, R., Inan, U., & Lyons, W. (2007). Very low frequency sferic bursts, sprites, and their association with lightning activity. *Journal of Geophysical Research*, *112*, D22105. https://doi.org/10.1029/2007JD008857

Mlynarczyk, J., Bor, J., Kulak, A., Popek, M., & Kubisz, J. (2015). An unusual sequence of sprites followed by a secondary TLE: An analysis of ELF radio measurements and optical observations. *Journal of Geophysical Research: Space Physics*, *120*, 2241–2254. https://doi.org/10.1002/2014JA020780

Nnadih, S., Kosch, M., Martinez, P., & Bor, J. (2018). First ground-based observations of sprites over southern Africa. *South African Journal of Science*, *9/10*, 1–6. https://doi.org/10.17159/sajs.2018/4272

Ohkubo, A., Fukunishi, H., Takahashi, Y., & Adachi, T. (2005). VLF/ELF sferic evidence for in-cloud discharge activity producing sprites. *Geophysical Research Letters*, *32*, L04812. https://doi.org/10.1029/2004GL021943

Parra-Rojas, F. C., Luque, A., & Gordillo-Vazquez, F. (2015). Chemical and thermal impacts of sprite streamers in the Earth's mesosphere. *Journal of Geophysical Research: Space Physics*, *120*, 8899–8933. https://doi.org/10.1002/2014JA020933

Pasko, V. (2010). Recent advances in theory of transient luminous events. *Journal of Geophysical Research*, *115*, A00E09. https://doi.org/10.1029/2009JA014860

Pasko, V., Inan, U., Bell, T., & Reising, S. (1998). Mechanism of ELF radiation from sprites. *Geophysical Research Letters*, *25*(18), 3493–3496. https://doi.org/10.1029/98GL02631

Pasko, V., Qin, J., & Celestin, S. (2013). Toward better understanding of sprite streamers: Initiation, morphology, and polarity asymmetry. *Surveys in Geophysics*, *34*, 797–830. https://doi.org/10.1007/s10712-013-9246-y

Picard, R., Inan, U., Pasko, V., Winick, J., & Wintersteiner, P. (1997). Infrared glow above thunderstorms?. *Geophysical Research Letters*, *24*(21), 2635–2638. https://doi.org/10.1029/97GL02753

Qin, J., Celestin, S., & Pasko, V. (2012). Minimum charge moment change in positive and negative cloud to ground lightning discharges producing sprites. *Geophysical Research Letters*, *39*, L22801. https://doi.org/10.1029/2012GL053951

Qin, J., Celestin, S., Pasko, V., Cummer, S., McHarg, G., & Stenbaek-Nielsen, H. (2013). Mechanism of column and carrot sprites derived from optical and radio observations. *Geophysical Research Letters*, *40*, 4777–4782. https://doi.org/10.1002/grl.50910

Reising, S., Inan, U., Bell, T., & Lyons, W. (1996). Evidence for continuing currents in sprite-producing lightning flashes. *Geophysical Research Letters*, *23*(24), 3639–3642. https://doi.org/10.1029/96GL03480

Romand, F., Vialatte, A., Croize, L., Payan, S., & Barthelemy, M. (2018). CO_2 thermal infrared signature following a sprite event in the mesosphere. *Journal of Geophysical Research: Space Physics*, *123*, 8039–8050. https://doi.org/10.1029/2018JA025894

Sentman, D., Wescott, E., Osborne, D., Hampton, D., & Heavner, M. (1995). Preliminary results from the Sprites94 aircraft campaign: 1. Red sprites. *Geophysical Research Letters*, *22*(10), 1205–1208. https://doi.org/10.1029/95GL00583

Soula, S., Mlynarczyk, J., Füllekrug, M., Peneda, N., Georgis, J.-F., van der Velde, O., et al. (2017). Dancing sprites: Detailed analysis of two case studies. *Journal of Geophysical Research: Atmospheres*, *122*, 3173–3192. https://doi.org/10.1002/2016JD025548

Taner, M., Koehler, F., & Sheriff, R. (1979). Complex seismic trace analysis. *Geophysics*, *44*(36), 1041–1063. https://doi.org/10.1190/1.1440994

University of Wyoming (2019). Upper air atmospheric soundings. http://weather.uwyo.edu/up-perair/sounding.html

Valdivia, J., Milikh, G., & Papadopoulos, K. (1997). Red sprites: Lightning as a fractal antenna. *Geophysical Research Letters*, *24*(24), 3169–3172. https://doi.org/10.1029/97GL03188

van der Velde, O., Mika, A., Soula, S., Haldoupis, C., Neubert, T., & Inan, U. (2006). Observations of the relationship between sprite morphology and in-cloud lightning processes. *Journal of Geophysical Research*, *111*, D15203. https://doi.org/10.1029/2005JD006879